JACS
JOURNAL OF THE AMERICAN CHEMICAL SOCIETY
pubs.acs.org/JACS
Communication

Divergent Adsorption Behavior Controlled by Primary Coordination Sphere Anions in the Metal−Organic Framework Ni_2X_2BTDD

Julius J. Oppenheim,[§] Jenna L. Mancuso,[§] Ashley M. Wright, Adam J. Rieth, Christopher H. Hendon,* and Mircea Dincă*

Cite This: https://doi.org/10.1021/jacs.1c07449

ABSTRACT: CO, ethylene, and H_2 demonstrate divergent adsorption enthalpies upon interaction with a series of anion-exchanged Ni_2X_2BTDD materials (X = OH, F, Cl, Br; H_2BTDD = bis(1*H*-1,2,3-triazolo[4,5-*b*][4′,5′-*i*])dibenzo[1,4]dioxin)). The dissimilar responses of these conventional π-acceptor gaseous ligands are in contrast with the typical behavior that may be expected for gas sorption in metal−organic frameworks (MOFs), which generally follows similar periodic trends for a given set of systematic changes to the host MOF structure. A combination of computational and spectroscopic data reveals that the divergent behavior, especially between CO and ethylene, stems from a predominantly σ-donor interaction between the former and Ni^{2+} and a π-acceptor interaction for the latter. These findings will facilitate further deliberate postsynthetic modifications of MOFs with open metal sites to control the equilibrium selectivity of gas sorption.

Gas sorption and separation studies continue to dominate research in metal−organic frameworks (MOFs) because a barrage of synthetic methods—including cation and linker exchange, postsynthetic functionalization of both the metal and linkers, and postsynthetic metalation of metallolinkers—allow fine-tuning of specific adsorbate−adsorbent interactions.[1−7] These aspects allow for the realization of high capacity, selective solid-state adsorbents for gas separations. In particular, MOF adsorbents have the potential to increase the efficiency of separations in which the relative volatility of the adsorbates is low.[8,9]

Deterministically tailoring frameworks with high sorption capacities to select for target species demands a detailed understanding of the structure−function relationships within the frameworks. One successful approach in this sense has been the use of MOFs with open metal sites (OMS) for the separation of gases that behave as π-acids from other gases that have weaker interactions with the metal sites.[10] The small-molecule binding affinity of OMS is governed by the adsorption geometry, orbital interactions, and relative electronegativity, which are in turn controlled by the MOF topology and composition. Prior investigations have focused on tuning adsorption strengths through direct metal substitution.[11] Modifications to the primary coordination sphere of OMS (through either steric hindrance or electronic perturbation) can have a substantial effect on the gas sorption properties.[12] For example, O_2 binds more strongly to $Co_2(OH)_2BBTA$ than to Co_2Cl_2BBTA (BBTA forms an framework isoreticular with that of the title Ni_2X_2BTDD), likely due to hydrogen-bonding interactions from the hydroxide as well as changes to the partial charge on the metal center enabling charge transfer to O_2.[13] Such studies are rare because modifications to a metal's primary coordination sphere can significantly alter the framework topology and be detrimental to porosity, crystallinity, or OMS accessibility.[14−16]

We sought to investigate the effect of the primary coordination sphere of the metal site on its interaction strength with the most relevant π-acid industrial gases: CO, ethylene, and H_2. These gases are components in some of the largest gas separation processes in industry.[1] Surprisingly, we find that, although all of these gases are traditionally classified as π-acids, their response to systematic anion exchanges in a single MOF host, Ni_2X_2BTDD, differs, spanning the broader range of σ-only through π-acid ligand field classifications. In these frameworks, the unique ability to tune the inner coordination sphere of a metal with an open coordination site allows for new insights into factors governing sorbate binding.

$Ni_2(OH)_2BTDD$ (**1-OH**), Ni_2F_2BTDD (**1-F**), Ni_2Cl_2BTDD (**1-Cl**), and Ni_2Br_2BTDD (**1-Br**) are isostructural and feature chains of alternating −M−X−M−X− units in the secondary building unit (SBU) (Figure 1). They can be synthesized following a literature procedure, by anion exchange from the parent **1-Cl**.[17] As has been previously reported, each of these frameworks remains crystalline upon anion exchange. Although the transformation is quantitative for **1-OH** and **1-Br**, fluoride exchange is substoichiometric, proceeding to the final formula $Ni_2F_{0.83}Cl_{0.17}BTDD$ for **1-F**.

To test the effect of the bridging anion on the binding strength of the three chosen adsorbates, we measured variable-temperature adsorption isotherms for activated samples of **1-X** (X = OH, F, Cl, Br) at 283, 288, 293, 298, and 308 K for CO

Received: July 17, 2021

https://doi.org/10.1021/jacs.1c07449
J. Am. Chem. Soc. XXXX, XXX, XXX−XXX

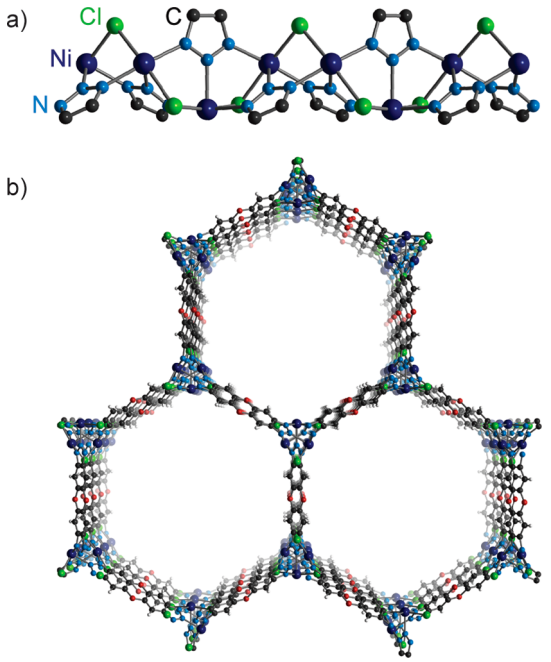

Figure 1. Portions of the X-ray crystal structure of Ni_2Cl_2BTDD (**1-Cl**): (a) the SBU viewed along the *c* axis; (b) view down the *c* axis.

and C_2H_4 and at 77 and 87 K for H_2. All experiments revealed type I isotherms (Figure 2).[18] The adsorbate coverage at 1 bar and 298 K is substoichiometric with respect to the metal sites, in ranges of 14−59% for CO and 43−75% for ethylene for the various **1-X** materials (Table 1). Given that the metal sites are likely the strongest adsorption sites in each MOF, deriving adsorption enthalpy data from these isotherms should provide sufficient information for comparative studies. The uptake capacity and OMS coverage is considerably reduced for **1-OH**, possibly indicating a weakened interaction between **1-OH** and each adsorbate. Finally, the H_2 capacity at 1 bar and 77 K is in excess of what would be expected for a stoichiometric M:H_2 interaction, with OMS coverage ranging from 174 to 252%, clearly indicating sorption on nonmetal sites.

ΔH_{ads} values were calculated using the Clausius−Clapeyron relation for the DSL, Sips, and Unilan models and directly for the Virial model. In order to exclude sources of error, ΔH_{ads} values were all interpolated at a coverage of 0.01 mmol/g (Section S6 in the Supporting Information). To specifically minimize systematic errors, enthalpy values were averaged over the results of all four fitting models (Figure 3a).[19] In transitions from F to Cl and Br, the $|\Delta H_{ads}|$ value for CO increases from 31 to 45 kJ/mol. The $|\Delta H_{ads}|$ value for **1-Br**, 45 kJ/mol, is large relative to those for similar MOFs, which typically range from 20 to 50 kJ/mol (Table S5.1). In contrast, $|\Delta H_{ads}|$ values for ethylene follow a reverse trend, decreasing from 33 to 20 kJ/mol on going from **1-F** to **1-Br**. An enthalpy of 20 kJ/mol is on the lower end for the interaction of ethylene with OMS MOFs, which typically falls between 20 and 60 kJ/mol (Table S5.2). The H_2 enthalpies are only weakly dependent upon the identity of the anion and fall between −7.0 and −7.6 kJ/mol. These values are only slightly larger than those observed for nonspecific adsorption (typically around −5 kJ/mol) and are on the lower end of what has been observed for MOFs with OMS, which typically range from −6 to −15 kJ/mol.[20−22] In the case of **1-OH**, a substantial decrease in the isosteric enthalpy of adsorption for both CO

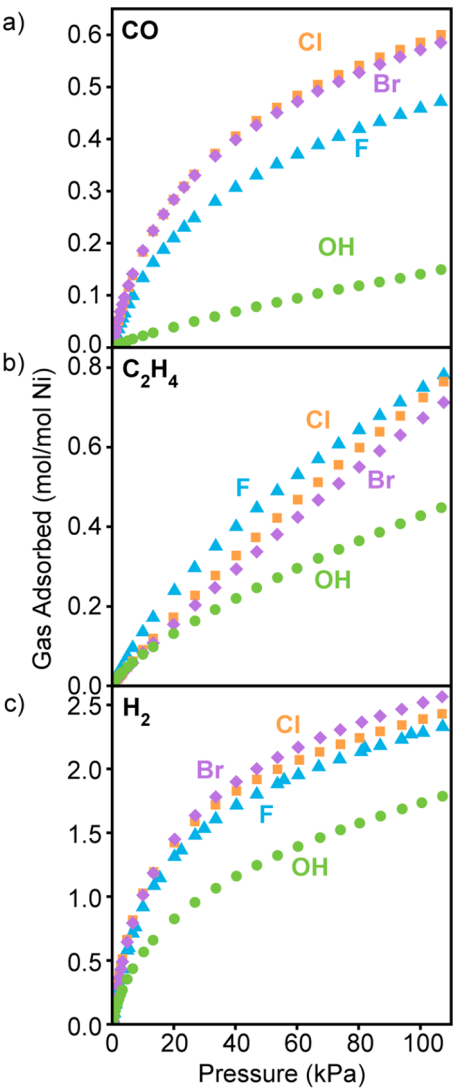

Figure 2. (a) CO (298 K), (b) ethylene (298 K), and (c) dihydrogen (77 K) adsorption isotherms for **1-X**.

Table 1. Summary of Adsorption Isotherm Data and Computational Binding Energies

gas	anion	total gas uptake capacity at 1 bar[a] (mol gas/mol BTDD)	open metal sites occupied at 1 bar[a] (%)	$-\Delta H_{ads}$ (kJ/mol)[b]	theoretical binding energy (HSEsol06)
CO	F[c]	0.92	46	31.00 ± 1.61	32.74
	Cl	1.17	59	39.02 ± 0.16	41.44
	Br	1.14	57	44.56 ± 0.75	44.42
	OH	0.29	14	16.42 ± 1.17	31.79
C_2H_4	F[c]	1.50	75	32.98 ± 0.40	25.07
	Cl	1.45	73	22.31 ± 0.24	23.62
	Br	1.35	67	19.80 ± 0.65	20.79
	OH	0.86	43	23.23 ± 1.14	13.06
H_2	F[c]	4.57	228	7.09 ± 0.02	9.78
	Cl	4.78	239	7.63 ± 0.01	12.90
	Br	5.04	252	7.62 ± 0.01	12.38
	OH	3.47	174	7.00 ± 0.01	13.83

[a]CO and ethylene at 298 K, H_2 at 77 K. [b]Averaged over Unilan, Virial, Sips, and Dual-Site Langmuir models. [c]Calculated for the experimental composition of $Ni_2F_{0.83}Cl_{0.17}BTDD$.

https://doi.org/10.1021/jacs.1c07449
J. Am. Chem. Soc. XXXX, XXX, XXX−XXX

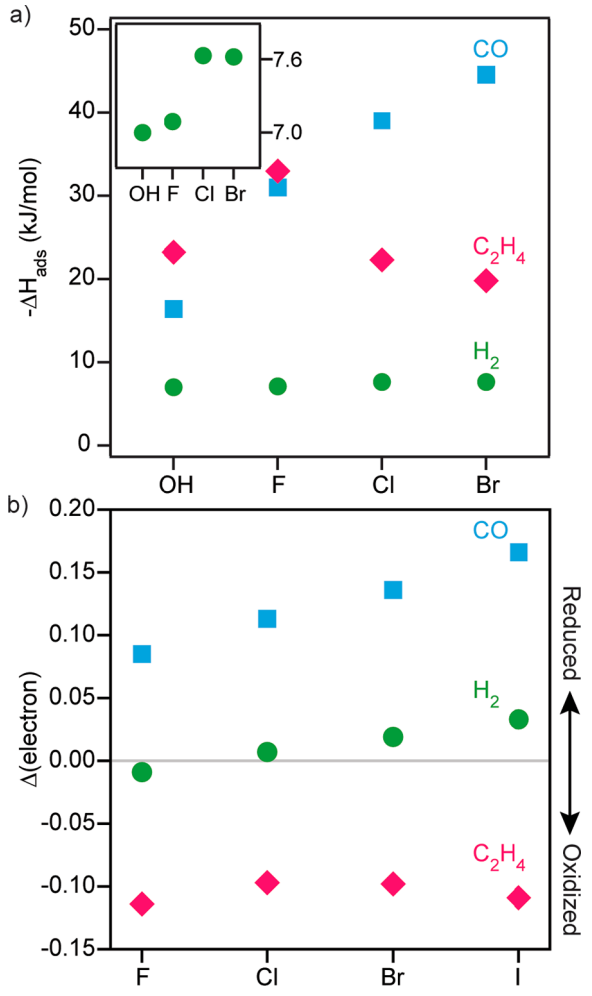

Figure 3. (a) Experimental isosteric enthalpies of adsorption for CO, ethylene, and hydrogen for **1-X** materials. Error bars are included in Table 1. Inset: magnified enthalpy axis for H_2 data. (b) DFT-calculated change in the total valence electrons on the nickel atom upon coordination of a sorbate.

and C_2H_4 is observed, accompanied by a large decrease in the uptake capacity. The decrease in uptake capacity suggests that access to the OMS is impeded (even though the material remains crystalline and porous to N_2) or that the hydroxide species have a complex interaction with these small molecules, such as the formation of hydrogen-bonding networks that could give rise to effective adsorbate−adsorbate repulsions.

To probe the type of bonding between CO and OMS, we used diffuse reflectance infrared Fourier transform spectroscopy (DRIFTS) to measure the CO bond stretching frequency upon dosing CO into **1-Cl**. The difference spectra (Figure 4; see also Figure S3.1) reveal a new band growing at 2170 cm^{-1} as the CO concentration increases. This frequency is higher than that for free CO (2143 cm^{-1}) and is indicative of a nonclassical metal−carbonyl interaction. This type of interaction has been previously noted in a series of structurally related M_2(dobdc) analogues (dobdc^{4-} = 2,5-dioxido-1,4-benzenedicarboxylate, M = Mg, Mn, Fe, Ni, Zn).[23] Nonclassical metal carbonyls typically involve a σ-bonding interaction (that causes a depletion of electron density from the antibonding HOMO of CO) with minimal or no π-back-donation to the CO π^* orbitals, resulting in strengthening of the C−O bond.[24] As such, the formally Ni(II) sites in

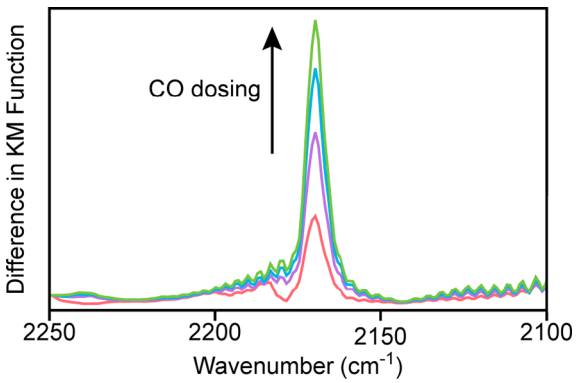

Figure 4. Difference in Kubelka−Munk intensities of DRIFTS data for **1-Cl** upon dosing with CO.

Ni_2X_2BTDD most likely do not participate as π-donors (or at least the d−π-interaction is insufficient to compete with the σ-interaction). It has been demonstrated, empirically, that the binding energy of nonclassical metal carbonyls has a linear relationship with the difference in energy between bound and free CO stretching frequencies ($\Delta\nu$).[25] Because the $\Delta\nu$ vs ΔH_{ads} point of **1-Cl** lies on this relationship, it is likely that the Ni−CO interaction is purely electrostatic (Figure S4.1). This provides further evidence that the increasing $|\Delta H_{ads}|$ values in the order **1-F** < **1-Cl** < **1-Br** is the direct result of the OMS becoming a stronger Lewis acid.

Electronic insights into the divergent adsorbate behaviors were obtained through periodic density functional theory (DFT) models at the HSEsol06 level, validated through agreement with the experimental $|\Delta H_{ads}|$ values (Figure S2.1). In interacting with the OMS, each gas adopts a different molecular orientation and orbital symmetry. Most significantly, exchange with the larger halogens bromide and (the theoretically predicted) iodide leads to an expansion of the SBU and consequent rotations of the BTDD linkers (Table S2.3), which in turn impedes access of ethylene to the metal site by blocking the most optimal d−π-overlap geometry (Figure S2.3). However, due to the terminal binding mode of CO and the small kinetic diameter of H_2, their binding is unperturbed by the geometric changes and steric limitations induced by anion exchange.

From an electronic perspective, an inspection of the partial charge density plots (Figure 5) for adsorbate binding reveals that the terminal binding mode of CO to Ni is dominated by σ-interactions, while the η^2-binding mode for ethylene has mostly π-character. Greater σ-donation from CO is also observed from the increase in electron density at the Ni site after binding, while the greater influence of π-back-bonding to ethylene induces partial oxidation of the metal center (Figure 3b). Further, as X is exchanged down the halogen group, the electron density on Ni upon binding CO increases, promoting the σ-donor interaction, while the electron density on Ni upon binding ethylene remains relatively constant. The increased capacity for σ-interaction is also revealed in the calculated density of states (DOS): with heavier halogens the conduction band shifts to more negative energies and is closer to the Fermi level (Figure S2.2). As the heavier halogens are weaker-field ligands, the d-orbitals that participate in the σ-interaction lie lower in energy and have greater energetic match with the σ-orbital of CO. This computational description supports the conclusion drawn from the infrared spectroscopy discussed

https://doi.org/10.1021/jacs.1c07449
J. Am. Chem. Soc. XXXX, XXX, XXX−XXX

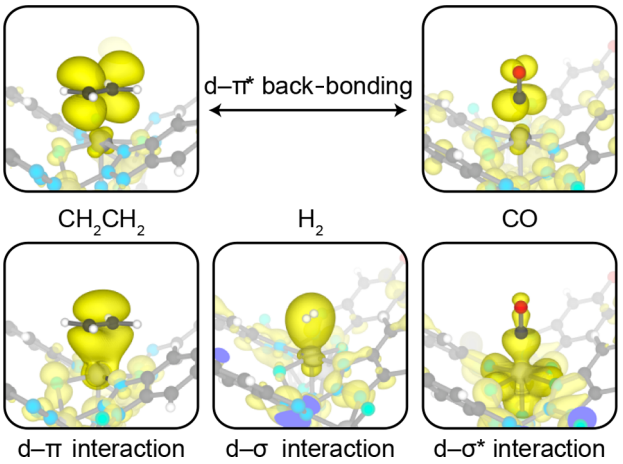

Figure 5. Charge density depictions of the electronic states associated with adsorbate binding, shown here for the Ni_2F_2BTDD derivative, revealing the divergent orbital interactions between MOF and molecules for ethylene (binding through the π-system), dihydrogen (binding through a σ-bond), and carbon monoxide (binding through a σ^*-orbital).

above, where the blue-shifted CO stretching frequency indicates a nonclassical metal carbonyl complex in which σ-interactions dominate. The partial charge density plots reveal that the Ni—H_2 interaction is of σ-symmetry and the electron density on Ni does not change significantly upon coordination of H_2, indicative of a weak interaction (Figure 3b).

In conclusion, we have probed the effect that anion exchange has on the interactions of three conventional π-acceptors with the open metal sites within Ni_2X_2BTDD. Surprisingly, we find that these gases display unique trends evidencing σ-donor, π-acceptor, and essentially nonspecific behavior. These results suggest that the subtle fine-tuning of metal sites enabled by postsynthetic changes to the primary coordination sphere, as opposed to the metal itself, can lead to a quantitative differentiation of gas interactions in MOFs with OMS, of potential utility for selective gas separations.

■ ASSOCIATED CONTENT

Supporting Information

The Supporting Information is available free of charge at https://pubs.acs.org/doi/10.1021/jacs.1c07449.

Supplementary figures and experimental details, including theoretical calculations and isosteric enthalpy of adsorption calculations (PDF)

■ AUTHOR INFORMATION

Corresponding Authors

Christopher H. Hendon − *Materials Science Institute, Department of Chemistry and Biochemistry, University of Oregon, Eugene, Oregon 97403, United States;* orcid.org/0000-0002-7132-768X; Email: chendon@uoregon.edu

Mircea Dincă − *Department of Chemistry, Massachusetts Institute of Technology, Cambridge, Massachusetts 02139, United States;* orcid.org/0000-0002-1262-1264; Email: mdinca@mit.edu

Authors

Julius J. Oppenheim − *Department of Chemistry, Massachusetts Institute of Technology, Cambridge, Massachusetts 02139, United States*

Jenna L. Mancuso − *Materials Science Institute, Department of Chemistry and Biochemistry, University of Oregon, Eugene, Oregon 97403, United States*

Ashley M. Wright − *Department of Chemistry, Massachusetts Institute of Technology, Cambridge, Massachusetts 02139, United States*

Adam J. Rieth − *Department of Chemistry, Massachusetts Institute of Technology, Cambridge, Massachusetts 02139, United States;* orcid.org/0000-0002-9890-1346

Complete contact information is available at: https://pubs.acs.org/10.1021/jacs.1c07449

Author Contributions

[§]J.J.O. and J.L.M. contributed equally.

Funding

This research was supported by the National Science Foundation through the Alan T. Waterman award to M. D. (DMR-1645232). Computational studies were performed by using the High- Performance Computing cluster at the University of Oregon (Talapas), the Extreme Science and Engineering Discovery Environment (XSEDE), which is supported by National Science Foundation Grant ACI-1548562, and the Portland State University machine, Coeus, which is supported by the NSF (DMS1624776). C.H.H. is supported in part by the National Science Foundation under Grant DMR-1956403, and the Research Corporation for Science Advancement (Cottrell Scholar Program) for non-tenured faculty.

Notes

The authors declare no competing financial interest.

■ REFERENCES

(1) Li, J.-R.; Kuppler, R. J.; Zhou, H.-C. Selective Gas Adsorption and Separation in Metal-Organic Frameworks. *Chem. Soc. Rev.* **2009**, *38* (5), 1477−1504.

(2) Kuppler, R. J.; Timmons, D. J.; Fang, Q.-R.; Li, J.-R.; Makal, T. A.; Young, M. D.; Yuan, D.; Zhao, D.; Zhuang, W.; Zhou, H.-C. Potential Applications of Metal-Organic Frameworks. *Coord. Chem. Rev.* **2009**, *253* (23), 3042−3066.

(3) Trickett, C. A.; Helal, A.; Al-Maythalony, B. A.; Yamani, Z. H.; Cordova, K. E.; Yaghi, O. M. The Chemistry of Metal-Organic Frameworks for CO 2 Capture, Regeneration and Conversion. *Nat. Rev. Mater.* **2017**, *2* (8), 1−16.

(4) Li, J.-R.; Sculley, J.; Zhou, H.-C. Metal-Organic Frameworks for Separations. *Chem. Rev.* **2012**, *112* (2), 869−932.

(5) You, W.; Liu, Y.; Howe, J. D.; Tang, D.; Sholl, D. S. Tuning Binding Tendencies of Small Molecules in Metal-Organic Frameworks with Open Metal Sites by Metal Substitution and Linker Functionalization. *J. Phys. Chem. C* **2018**, *122* (48), 27486−27494.

(6) Sours, T.; Patel, A.; Nørskov, J.; Siahrostami, S.; Kulkarni, A. Circumventing Scaling Relations in Oxygen Electrochemistry Using Metal-Organic Frameworks. *J. Phys. Chem. Lett.* **2020**, *11* (23), 10029−10036.

(7) Poloni, R.; Lee, K.; Berger, R. F.; Smit, B.; Neaton, J. B. Understanding Trends in CO2 Adsorption in Metal-Organic Frameworks with Open-Metal Sites. *J. Phys. Chem. Lett.* **2014**, *5* (5), 861−865.

(8) Sholl, D. S.; Lively, R. P. Seven Chemical Separations to Change the World. *Nature* **2016**, *532* (7600), 435.

(9) Hinchliffe, A.; Porter, K. A Comparison of Membrane Separation and Distillation. *Chem. Eng. Res. Des.* **2000**, *78* (2), 255−268.

(10) Kökcam-Demir, Ü.; Goldman, A.; Esrafili, L.; Gharib, M.; Morsali, A.; Weingart, O.; Janiak, C. Coordinatively Unsaturated

Metal Sites (Open Metal Sites) in Metal-Organic Frameworks: Design and Applications. *Chem. Soc. Rev.* **2020**, *49* (9), 2751−2798.
(11) Rieth, A. J.; Tulchinsky, Y.; Dincă, M. High and Reversible Ammonia Uptake in Mesoporous Azolate Metal-Organic Frameworks with Open Mn, Co, and Ni Sites. *J. Am. Chem. Soc.* **2016**, *138* (30), 9401−9404.
(12) Barnett, B. R.; Parker, S. T.; Paley, M. V.; Gonzalez, M. I.; Biggins, N.; Oktawiec, J.; Long, J. R. Thermodynamic Separation of 1-Butene from 2-Butene in Metal-Organic Frameworks with Open Metal Sites. *J. Am. Chem. Soc.* **2019**, *141* (45), 18325−18333.
(13) Rosen, A. S.; Mian, M. R.; Islamoglu, T.; Chen, H.; Farha, O. K.; Notestein, J. M.; Snurr, R. Q. Tuning the Redox Activity of Metal-Organic Frameworks for Enhanced, Selective O2 Binding: Design Rules and Ambient Temperature O2 Chemisorption in a Cobalt-Triazolate Framework. *J. Am. Chem. Soc.* **2020**, *142* (9), 4317−4328.
(14) Sun, L.; Hendon, C. H.; Minier, M. A.; Walsh, A.; Dincă, M. Million-Fold Electrical Conductivity Enhancement in Fe2(DEBDC) versus Mn2(DEBDC) (E = S, O). *J. Am. Chem. Soc.* **2015**, *137* (19), 6164−6167.
(15) Li, D.; Nielsen, M. H.; Lee, J. R.; Frandsen, C.; Banfield, J. F.; De Yoreo, J. J. Direction-Specific Interactions Control Crystal Growth by Oriented Attachment. *Science* **2012**, *336* (6084), 1014−1018.
(16) Gygi, D.; Bloch, E. D.; Mason, J. A.; Hudson, M. R.; Gonzalez, M. I.; Siegelman, R. L.; Darwish, T. A.; Queen, W. L.; Brown, C. M.; Long, J. R. Hydrogen Storage in the Expanded Pore Metal-Organic Frameworks M2(Dobpdc) (M = Mg, Mn, Fe, Co, Ni, Zn). *Chem. Mater.* **2016**, *28* (4), 1128−1138.
(17) Rieth, A. J.; Wright, A. M.; Skorupskii, G.; Mancuso, J. L.; Hendon, C. H.; Dincă, M. Record-Setting Sorbents for Reversible Water Uptake by Systematic Anion Exchanges in Metal-Organic Frameworks. *J. Am. Chem. Soc.* **2019**, *141* (35), 13858−13866.
(18) Thommes, M.; Kaneko, K.; Neimark, A. V.; Olivier, J. P.; Rodriguez-Reinoso, F.; Rouquerol, J.; Sing, K. S. Physisorption of Gases, with Special Reference to the Evaluation of Surface Area and Pore Size Distribution (IUPAC Technical Report). *Pure Appl. Chem.* **2015**, *87* (9−10), 1051−1069.
(19) Nuhnen, A.; Janiak, C. A Practical Guide to Calculate the Isosteric Heat/Enthalpy of Adsorption via Adsorption Isotherms in Metal-Organic Frameworks, MOFs. *Dalton Transactions* **2020**, *49* (30), 10295−10307.
(20) Kapelewski, M. T.; Runcevski, T.; Tarver, J. D.; Jiang, H. Z. H.; Hurst, K. E.; Parilla, P. A.; Ayala, A.; Gennett, T.; FitzGerald, S. A.; Brown, C. M.; Long, J. R. Record High Hydrogen Storage Capacity in the Metal-Organic Framework Ni2 (m-Dobdc) at near-Ambient Temperatures. *Chem. Mater.* **2018**, *30* (22), 8179−8189.
(21) Rosnes, M. H.; Opitz, M.; Frontzek, M.; Lohstroh, W.; Embs, J. P.; Georgiev, P. A.; Dietzel, P. D. Intriguing Differences in Hydrogen Adsorption in CPO-27 Materials Induced by Metal Substitution. *J. Mater. Chem. A* **2015**, *3* (9), 4827−4839.
(22) Areán, C. O.; Chavan, S.; Cabello, C. P.; Garrone, E.; Palomino, G. T. Thermodynamics of Hydrogen Adsorption on Metal-Organic Frameworks. *ChemPhysChem* **2010**, *11* (15), 3237−3242.
(23) Bloch, E. D.; Hudson, M. R.; Mason, J. A.; Chavan, S.; Crocellà, V.; Howe, J. D.; Lee, K.; Dzubak, A. L.; Queen, W. L.; Zadrozny, J. M.; et al. Reversible CO Binding Enables Tunable CO/H2 and CO/N2 Separations in Metal-Organic Frameworks with Exposed Divalent Metal Cations. *J. Am. Chem. Soc.* **2014**, *136* (30), 10752−10761.
(24) Hadjiivanov, K. I.; Panayotov, D. A.; Mihaylov, M. Y.; Ivanova, E. Z.; Chakarova, K. K.; Andonova, S. M.; Drenchev, N. L. Power of Infrared and Raman Spectroscopies to Characterize Metal-Organic Frameworks and Investigate Their Interaction with Guest Molecules. *Chem. Rev.* **2021**, *121* (3), 1286−1424.
(25) Zecchina, A.; Scarano, D.; Bordiga, S.; Spoto, G.; Lamberti, C. Surface Structures of Oxides and Halides and Their Relationships to Catalytic Properties. *Adv. Catal.* **2001**, *46*, 265−397.

https://doi.org/10.1021/jacs.1c07449
J. Am. Chem. Soc. XXXX, XXX, XXX−XXX